Cytotoxic and antimicrobial mycophenolic acid derivatives from an endophytic fungus *Penicillium* sp. MNP-HS-2 associated with *Macrozamia communis*

Mohamed S. Elnaggar[1,*,#], Nehal Ibrahim[1,*,#], Ahmed M. Elissawy[1], Alaa Anwar[1], Mahmoud A. A. Ibrahim[2,3], Sherif S. Ebada[1,*]

[1]Department of Pharmacognosy, Faculty of Pharmacy, Ain Shams University, Abbassia, 11566, Cairo, Egypt.

[2]Computational Chemistry Laboratory, Chemistry Department, Faculty of Science, Minia University, Minia 61519, Egypt.

[3]School of Health Sciences, University of KwaZulu-Natal, Westville, Durban 4000, South Africa.

* Correspondence:

E-mail: mohamed.s.elnaggar@pharma.asu.edu.eg (M.S.E.), Tel.: +20-2405-1180, Fax: +20-2405-1107; nehal.sabry@pharma.asu.edu.eg (N.I.), Tel.: +20-2405-1180, Fax: +20-2405-1107; sherif.elsayed@helmholtz-hzi.de; sherif_elsayed@pharma.asu.edu.eg (S.S.E.); Tel.: +49-531-6181-4223, Fax: +49-531-6181-9499

[#] These authors contributed equally to this work.

Abstract

Macrozamia communis and its associated endophytic fungi are untapped sources of bioactive metabolites with great potential for medicinal exploitation. Chemical investigation of the mycelial extract derived from an endophytic fungus *Penicillium* sp. MNP-HS-2 associated with *M. communis* fruit offered four mycophenolic acid derivatives recognized as previously undescribed natural products (**1**-**4**) together with nine known metabolites (**5**-**13**). Chemical structures of isolated compounds were determined based on extensive spectroscopic analyses, including 1D/2D NMR and HRESIMS. The absolute stereochemistry of alternatain E (**1**) was unambiguously established by comparing its experimental and calculated time-dependent density functional theory electronic circular dichroism spectra (TDDFT-ECD). All isolated compounds were assessed for their antimicrobial and cytotoxic activities, where mycophenolic acid methyl ester (**7**) displayed significant cytotoxic activity against seven different cell lines with IC_{50} values in the low micromolar to nanomolar range, whereas mycophenolene A (**3**) exhibited a potent antibacterial activity against *Staphylococcus aureus* (MIC = 2.1 µg/mL).

Keywords: *Macrozamia*; *Penicillium*; endophyte; mycophenolic acid; cytotoxic; antibacterial.

1. Introduction

Endophytes exist in all ecological niches on earth and hold an immense promise to the bio-prospection and sustainable production of previously undescribed chemical entities for countless applications (Amr et al., 2023). The last few decades have witnessed a growing interest in fungal endophytes as an omnipresent and a versatile source of bioactive metabolites, especially anti-infective and cytotoxic compounds. These interests are supported by the current exploitation of botanical resources, which could lead to their exhaustion with heavy ecological burden (Zhu et al., 2021). With over 350 species, *Penicillium* represents one of the largest fungal genera present in the mycobiome of many organisms (Visagie et al., 2014). Although *Penicillium* species have been well recognized as a source of antibiotics, they displayed myriads of pharmacological activities far beyond their antibiotic production potential, including antidiabetic, anticancer, antifibrotic and immunosuppressive activities (Toghueo and Boyom, 2020).

Macrozamia communis L.A.S. Johnson is a Zamiaceae cycad endemic to eastern Australia (New South Wales). The plant was locally known as 'burrawang' by Australian aborigines who considered the fresh seeds to be toxic and consumed them as bush food only after processing them by water leaching or burying (fermentation) (Asmussen, 2012). Although the detoxification treatment performed by aborigines (one-month burial) suggests a potential role of endophytes, rare biological and chemical studies on *M. communis* or its endophytes have been traced. Hence, in this study we chemically investigated an *M. communis*-derived endophytic fungus *Penicillium* sp. MNP-HS-2 to elaborate its bioactive secondary metabolites offering four previously undescribed natural products (**1**-**4**) together with nine known metabolites (**5**-**13**). In this study, we report isolation and structure elucidation of compounds **1**-**13** in addition to their antimicrobial and cytotoxic potentials.

2. Results and discussion

2.1. Chemical investigation of fungal ethyl acetate extract

The culture extract of the ascomycete endophyte *Penicillium* sp. MNP-HS-2, derived from *M. communis* fruit, was purified using chromatographic techniques to yield four previously undescribed natural products (**1-4**), in addition to nine known metabolites (**5-13**) (Figure 1) namely; isoeuparvic acid (**5**) (Zhang et al., 2018), its methyl ester (**6**) (Xu et al., 2017), mycophenolic acid methyl ester (**7**) (Elsebai, 2021), two isocoumarin derivatives (**8** and **9**) (Kimura et al., 2007; Wang et al., 2012), terreusinone A (**10**) (Wei et al., 2015), isoochracinate A2 (**11**) (Pang et al., 2018), alternarian acid (**12**) (Chadwick et al., 1984), and alternatain B (**13**) (Yang et al., 2019).

Compound **1** was isolated as a white amorphous solid. Its molecular formula was established to be $C_{13}H_{10}O_6$ based on HRESIMS that illustrated a protonated molecule at *m/z* 263.0548 $[M+H]^+$ (calculated for 263.0546) and a sodium adduct at *m/z* 285.0369 $[M+Na]^+$ (calculated for 285.0367), indicating nine degrees of unsaturation. The ^{13}C NMR spectral data of **1** (Table 1, Figure S4) exhibited the presence of eight unprotonated carbon atoms, including two carbonyl groups (δ_c 169.4, 166.2), five olefinic carbon atoms (δ_c 168.8, 164.1, 161.5, 147.2, 105.4) and a deshielded aliphatic carbon (δ_c 108.6), suggesting its existence as a hemiacetal carbon. In addition, the ^{13}C NMR spectrum of **1** showed three tertiary olefinic carbons (δ_c 120.1, 105.5, 99.7) and two primary carbons, including one olefinic methyl (δ_c 11.9) and a methoxy group (δ_c 56.6). The interpretation of ^{13}C NMR data of **1** accounted for six degrees of unsaturation suggesting that compound **1** has a tricyclic structure. Based on the obtained results and by comparison to the reported literature (Aly et al., 2008; Liu et al., 2016; Yang et al., 2019), compound **1** was proposed to be a polyketide

altenusin derivative with 6/5/5 ring scaffold. Further confirmation of the depicted structure of **1** (Figure 1) was provided by 2D NMR, including ^{1}H-^{1}H COSY, HMBC and ROESY (Table 1, Figure 2). The ^{1}H-^{1}H COSY spectrum of **1** revealed two long-range spin systems, one extending over two *meta*-coupled aromatic protons at δ_H 6.59 (H-4) and at δ_H 6.55 (H-6) and another extending between one olefinic proton at δ_H 6.29 (H-10) and a methyl group at δ_H 1.92 (H_3-12). The HMBC spectrum of **1** (Table 1, Figure 2) showed key correlations from olefinic methyl group at δ_H 1.92 ppm to four carbons at δ_c 169.4 (C-11), δ_c 164.1 (C-9), δ_c 120.1 (C-10) and δ_c 108.6 (C-8), indicating its presence on an olefinic bond in a lactone ring. The HMBC spectrum also revealed key correlations from a methoxy group at δ_H 3.86 (OCH_3-13) and two *meta*-coupled aromatic protons at δ_H 6.59 (H-4) and at δ_H 6.55 (H-6) to an oxygenated aromatic carbon at δ_C 168.8 (C-5), indicating that the methoxy group was positioned at C-5. In addition, the HMBC spectrum also revealed key correlations from H-4 to a carbonyl carbon at δ_C 166.2 (C-1) and an oxygenated olefinic carbon at δ_C 161.5 (C-3), confirming the proposed ring structure for **1**. The ROESY spectrum of **1** (Table 1, Figure 2) further supported its structure by revealing key NOE correlations from H-10 to H_3-12 and from both *meta*-coupled aromatic protons H-4/H-6 to a methoxy group (OCH_3-13).

The absolute configuration of **1** was established by comparing experimental and TDDFT-simulated ECD spectra. All possible conformations of **1** within energy window of 10 kcal mol^{-1} were generated and optimized at B3LYP/6-31G* level of theory. The first 50 excitation states were then computed based on time-dependent density-functional theory (TDDFT) at B3LYP/6-31G* level in methanol by the PCM model. The generated TDDFT-ECD spectra were Boltzmann-weighted and compared to the experimental spectrum (Figure 3). The TDDFT-simulated ECD spectrum was in a good agreement with its corresponding experimental ECD

spectra (Figure 3). This comparison revealed the absolute configuration of C-8 is assigned as *R*-configuration. According to the aforementioned results, compound **1** was deduced to be a previously undescribed polyketide altenusin derivative, structurally following alternatain A (Yang et al., 2019) and talaroflavone (Ayer and Racok, 1990), with a major difference of having two spiro-oriented lactone rings, and hence was trivially named alternatain E.

Compound **2** was purified as an off-white amorphous solid and its molecular formula was determined to be $C_{18}H_{20}O_6$ based on HRESIMS that revealed a protonated molecule at *m/z* 333.1341 $[M+H]^+$ (calculated 333.1340) and a sodium adduct at *m/z* 355.1159 $[M+Na]^+$ (calculated 355.1158), indicating nine degrees of unsaturation. The ^1H and ^{13}C NMR spectrum of **2** (Table S1) revealed the presence of two *cis*-oriented olefinic protons at δ_H 6.69 (d, *J*= 10.2 Hz, H-1'; δ_C 118.8) and at δ_H 5.73 (d, *J*= 10.2 Hz, H-2'; δ_C 130.1), along with the characteristic proton resonances of mycophenolic acid skeleton, including a singlet methylene group at δ_H 5.21 (H_2-3; δ_C 70.1), an olefinic methyl group at δ_H 2.13 (H_3-8; δ_C 10.8) and a singlet aromatic methoxy group at δ_H 3.80 (H_3-9; δ_C 62.2). A literature search of compound **2** based on the obtained results and the reported mycophenolic acid derivatives suggested it was similar to mycochromenic acid that was previously reported as a fungal biotransformation metabolite (Xu et al., 2017) and as a synthetic product (Yamaguchi et al., 2006). The major difference between **2** and mycochromenic acid is the presence of an additional methoxy group at δ_H 3.62 (H_3-7'; δ_C 52.1) that was correlated by HMBC spectrum (Figure 4) to a carboxyl carbon at δ_C 175.5 (C-6'), indicating its identity as mycochromenic acid methyl ester and accounting for the higher molecular weight of **2** by 14 amu. Compound **2** was only reported as a synthetic product (Yamaguchi et al., 2006). To the best of our knowledge, this is the first report of **2** as a natural fungal metabolite. It is noteworthy to mention that while mycochromenic acid methyl ester (**2**) was a major product in the explored extract, its

free acid was not detected in either total extract or its subsequent fractions. In addition, during preparative HPLC separations, acetonitrile, rather than methanol, was used as a polar solvent. This observation supports that mycochromenic acid methyl ester (**2**), in this study, is obtained as a genuine fungal metabolite and not as an artefact emerging during the chromatographic workup. The absence of optical rotation value ($[\alpha]_{D}^{20}$ 0 (*c* 0.2, acetonitrile)) of **2** indicated that it was isolated as a racemic mixture whose separation was unsuccessful using the available facilities.

Compounds (**3** and **4**) were obtained as white amorphous solids and their molecular formulas were established to be $C_{24}H_{32}O_4$ and $C_{25}H_{34}O_4$ based on HRESIMS analyses that demonstrated protonated molecules at *m/z* 385.2374 $[M+H]^+$ (calculated 385.2373) and at *m/z* 399.2530 $[M+H]^+$ (calculated 399.2528), respectively. The ^1H and ^{13}C NMR data of **3** and **4** (Table S2, S3) revealed similar patterns of proton and carbon resonances that, by comparison with the reported literature, were found to be following the chemical structure of 6-*trans*,*trans*-farnesyl-5,7-dihydroxy-4-methylphthalide lacking detailed description of its NMR spectral data (Canonica et al., 1972). The ^1H and ^{13}C NMR data of **3** (Table S2) were assigned based on 2D NMR spectral analysis, including ^1H-^1H COSY, HMBC and HMQC. Compound **3** was trivially named mycophenolene A. The ^1H NMR data of **4** (Table S3) displayed an additional singlet oxygenated methyl group at δ_H 3.80 (H_3-9; δ_C 61.3) compared to **3**, explaining its higher molecular weight by 14 amu. The HMBC spectrum of **4** confirmed the position of the additional methoxy group to be at C-5 (δ_C 164.4), which in turn was also correlated with an aromatic methyl at δ_H 2.16 (H_3-8), a singlet methylene at δ_H 5.30 (H_2-3) and a doublet methylene at δ_H 3.40 (H_2-1'). Based on the obtained results, compound **4** was unambiguously identified as a previously undescribed natural 5-methoxy derivative of **3** and it was trivially named mycophenolene B.

2.2. In vitro antimicrobial evaluation of the isolated compounds

The isolated compounds were evaluated for their antimicrobial activity against a panel of twelve microorganisms, including Gram-positive, Gram-negative bacteria and fungi (Table 2). Four compounds revealed moderate to weak antimicrobial activities (MIC ≥ 66.6 µg/mL) (Table 2). Among the tested compounds, mycophenolene A (**3**) demonstrated potent antibacterial activity against *S. aureus* (MIC= 2.1 µg/mL), while its methyl ether **(4)** showed no activity, in spite of possessing the same substitution pattern on phthalide ring as mycophenolic acid, previously known for its antibacterial activity (Siebert et al., 2018). This notion suggests that the free phenolic 5-OH moiety of mycophenolene A **(3)** may contribute to the antibacterial activity and concurs with the formerly reported results of anti-*Staphylococcus aureus* activity of resorcinol derivatives (Joray et al., 2011). Indeed, the presence of two phenolic OH groups was found to be essential for antimicrobial activity through ATP synthase inhibition (Narang et al., 2019). Mycophenolic acid methyl ester (**7**) showed weak antimicrobial action against *M. smegmatis* and the tested fungal strains in accordance with a previous report (Siebert et al., 2018).

2.3. In vitro cytotoxic evaluation of the isolated compounds

The isolated compounds were tested for their cytotoxic activity against seven different cell lines. The obtained results (Table 3) disclosed that mycophenolic acid methyl ester (**7**) possesses a significant pan-cytotoxic activity against all tested cell lines (IC_{50} ranging from 0.1 to 0.4 µM). Cancer-specific susceptibility to mycophenolic acid methyl ester was not observed among the tested cell lines as previously reported for the parent compound mycophenolic acid (Benjanuwattra et al., 2020). Mycophenolic acid, initially recognized as an immunosuppressant, was repurposed for anticancer chemotherapy research with potent anticancer activity against various malignancies (Benjanuwattra et al., 2020).

Compound **3** (mycophenolene A) displayed potent cytotoxic activity against the human cervix carcinoma cell line (KB3.1) with IC_{50} of 8.3 µM. Meanwhile, the inactivity of compound **4** implies that methylation of 5-OH leads to the loss of activity, in distinction from the reported crucial role of 5-OMe in mycophenolic acid cytotoxicity (Mitsuhashi et al., 2010). This suggests that **3** exerts its cytotoxic activity via a mechanism different from that of mycophenolic acid and encourages future pharmacomodulation studies on the phthalide and polyene moieties of **3**. Indeed, it was formerly stated that changes in the alkyl chain of mycophenolic acid improved histone deacetylase (HDAC) inhibitory activity at the expense of its inosine-5'-monophosphate dehydrogenase-2 (IMPDH2) inhibition (Mitsuhashi et al., 2010). Among the tested compounds, isoochracinate A2 (**11**) (Table 3) revealed potent antiproliferative activities against MCF-7 (breast), PC-3 (prostate) and L929 (fibroblast) cell lines, with IC_{50} values of 3.6, 11.3 and 12.6 µM, respectively.

Among the tested compounds, only **3**, **5**, **6**, **7** and **11** revealed antimicrobial and/or cytotoxic activities. In particular, mycophenolic acid methyl ester (**7**) displayed potent cytotoxic activity against all tested cell lines and moderate to weak antimicrobial action against four of the tested strains. The prolific ability of endophytes to produce antimicrobial and cytotoxic metabolites can be regarded as a tool to inhibit the growth of competing organisms and hence, to maintain their microenvironment (Gao et al., 2018). However, these metabolites of significant antimicrobial and/or cytotoxicity offer a great opportunity to enrich Drug Discovery Pipeline with previously undescribed scaffolds that in turn might be potential to develop lead molecules for new pharmaceuticals.

3. Conclusion

Fungal endophytes are a ubiquitous versatile source for the bio-prospection of unprecedentedly reported chemical scaffolds with countless applications. This study aimed at exploring the

associated fungal endophytes within *M. communis* fruit. The metabolic profile of genus *Penicillium* was enriched by four previously undescribed phthalide derivatives, including a unique spiroketal phthalide, together with nine known metabolites. Among the isolated metabolites, some displayed significant anticancer potential such as mycophenolene A (**3**), mycophenolic acid methyl ester (**7**) and isoochracinate A2 (**11**). The former proved strong anti-*Staphylococcus aureus* activity. Further in-depth investigation of the active compounds will be a subject for future research to interpret their mechanism of action and to achieve their full medicinal potential.

4. Materials & methods

4.1. General Experimental Procedure

Optical rotation measurement was performed in acetonitrile (Uvasol, Merck, Darmstadt, Germany) at 20 °C using Anton Paar MCP-150 polarimeter (Seelze, Germany). UV/vis spectra were obtained in methanol (Uvasol, Merck, Darmstadt, Germany) using UV/Vis 2450 spectrophotometer (Shimadzu, Kyoto, Japan). ECD spectra were recorded on a J-815 spectropolarimeter (JASCO, Pfungstadt, Germany). The NMR spectra were recorded on Avance III 500 spectrometer (^{1}H NMR, 500 MHz; and ^{13}C NMR, 125 MHz, Bruker) and on Avance 700 spectrometer equipped with 5 mm TXI cryoprobe (Bruker, ^{1}H NMR, 700 MHz; and ^{13}C NMR, 175 MHz). UltiMate 3000 Series UHPLC (Thermo Fischer Scientific, Waltman, MA) equipped with an amaZon speed ESI-Iontrap-MS (Bruker, Billerica, MA) was employed to record the ESI-MS spectra using a C18 Acquity UPLC BEH column (2.1 × 50 mm, 1.7 µm) (Waters, Milford, MA). The HPLC and diode-array detector (DAD) conditions were set as previously published (Becker et al., 2020). Agilent 1200 Infinity Series HPLC instrument (Agilent Technologies, Santa Clara, CA) was used for high-resolution electrospray ionization mass spectrometry (HRESIMS) analyses using the same column

and applying the same solvent composition and elution system as above. UV/vis detection (200−640 nm) was connected to maXis ESI-TOF mass spectrometer (Bruker) using the following parameters: scan range 100−2500 m/z, capillary voltage 4500 V, dry temperature 200 °C. The final purification steps of metabolites were performed on Agilent 1100 preparative HPLC (Agilent, Waldbronn, Germany). All chemicals were procured by Carl Roth GmbH (Karlsruhe, Germany) and AppiChem GmbH (Darmstadt, Germany), whereas solvents for HPLC runs were purchased from Merck (Darmstadt, Germany).

4.2. Fungal Material and identification

A female strobile (40 × 20 cm) of *M. communis* was collected from Hunter Region Botanic Gardens (New South Wales, Australia) and was kindly authenticated by Prof. Ken Page. According to the standard protocols, the fungal strain was isolated from the inner tissues of the fruit. The fruit was rinsed thoroughly with distilled water then subjected to surface sterilization by dipping in 70% ethanol for 2 min and small pieces from the inner tissues were cut using sterilized blade and placed onto malt agar plate (15 g/L malt extract, 15 g/L agar, 0.2 g/L chloramphenicol to suppress bacterial growth, pH adjusted to 7.4-7.8 using 10% NaOH). By regular inspection of the incubated plate at 25°C, the investigated fungal strain was observed to grow out of the fruit tissues. Then, pure fungal strain was grown by repeated re-inoculation on fresh culture media.

4.3. Identification of the fungal strain

The fungal strain in this study was identified as *Penicillium* sp. MNP-HS-2 using a molecular biological protocol by DNA amplification and sequencing of the ITS region as previously described (Kjer et al., 2010). The sequencing data were submitted to the GenBank with an accession number OQ780796.

4.4. Cultivation, extraction and isolation

Erlenmeyer flasks (20 × 1 L) containing rice (100 g) and water (110 mL) were set aside overnight, then autoclaved (20 min at 121 °C), and used for fermentation of the fungal biomass on solid rice medium at 25 °C for six weeks under static conditions. For harvesting, each flask was soaked in EtOAc (500 mL), and the culture mass was mechanically cut into small pieces by a spatula. The flasks were set aside overnight then shaken for 8 h at 150 rpm. The combined EtOAc extracts were then evaporated in vacuum at 40 ºC to yield brown oily residue. The obtained residue was suspended in 90% aqueous methanol and partitioned with *n*-hexane, yielding dark brown crude extract (7.0 g). The defatted extract was subjected to normal phase preparative HPLC (60 g silica gel) applying gradient elution using *n*-heptane:dichloromethane (100:0 to 0:100) followed by dichloromethane:methanol (100:0-0:100) yielding twenty-two fractions (1-22) that were analyzed using LCMS. Selected fractions were then purified using preparative HPLC revered phase (RP) applying isocratic elution using water:acetonitrile as a mobile phase. Fraction 11 (26 mg) was purified using 75% acetonitrile in water to yield compounds **3** (1.5 mg, t_R = 26 min) and **4** (1.5 mg, t_R = 38 min). Fraction 13 (87 mg) was purified using 55% acetonitrile in water yielding compounds **5** (1.0 mg, t_R = 12 min)**, 6** (2.0 mg, t_R = 19 min) and **7** (80 mg, t_R = 25 min). Similarly, fraction 14 (73 mg) was purified using 45 % acetonitrile in water to yield compounds **11** (4.0 mg, t_R = 7 min) and **8** (1.0 mg, t_R = 14 min). Fraction 16 (94 mg) was fractionated using 45 % acetonitrile in water to yield compounds **1** (3.0 mg, t_R = 6 min), **2** (10.0 mg, t_R = 14 min), **9** (3.5 mg, t_R = 16 min) and **10** (1.5 mg, t_R = 21 min). Fraction 22 was purified using 30% acetonitrile in water to yield compounds **12** (2.5 mg, t_R = 13 min) and **13** (2.5 mg, t_R = 8 min).

4.5. Compounds characterization

*4.5.1. Alternatain E (**1**)*: White amorphous solid; $[\alpha]_D^{20}$ +2.1 (*c* 0.2, acetonitrile); UV (MeOH) λ_{max} 219, 264, and 300 nm; ^{1}H and ^{13}C NMR see Table 1; in LRESIMS *m/z* 263.02 $[M+H]^+$, 285.02 $[M+Na]^+$ and at *m/z* 260.97 $[M-H]^-$; HRESIMS *m/z* 263.0548 $[M+H]^+$ (calculated for $C_{13}H_{11}O_6$; 263.0546) and at *m/z* 285.0369 $[M+Na]^+$ (calculated for $C_{13}H_{10}NaO_6$; 285.0367).

*4.5.2. Mycochromenic acid methyl ester (**2**)*: Off-white amorphous solid; $[\alpha]_D^{20}$ 0 (*c* 0.2, acetonitrile); UV (MeOH) λ_{max} 201, 248 and 334 nm; ^{1}H and ^{13}C NMR see Table S1; in LRESIMS *m/z* 333.15 $[M+H]^+$ and *m/z* 331.12 $[M-H]^-$; HRESIMS *m/z* 333.1341 $[M+H]^+$ (calculated for $C_{18}H_{21}O_6$; 333.1340) and *m/z* 355.1159 $[M+Na]^+$ (calculated for $C_{18}H_{20}NaO_6$; 355.1158).

*4.5.3. Mycophenolene A (**3**)*: White amorphous solid; UV (MeOH) λ_{max} 220, 260 and 298 nm; ^{1}H and ^{13}C NMR see Table S2; in LRESIMS *m/z* 385.24 $[M+H]^+$ and *m/z* 383.20 $[M-H]^-$; HRESIMS *m/z* 385.2374 $[M+H]^+$ (calculated for $C_{24}H_{33}O_4$; 385.2373) and *m/z* 407.2195 $[M+Na]^+$ (calculated for $C_{24}H_{32}NaO_4$; 407.2194).

*4.5.4. Mycophenolene B (**4**)*: White amorphous solid; UV (MeOH) λ_{max} 220 and 298 nm; ^{1}H and ^{13}C NMR see Table S3; in LRESIMS *m/z* 399.28 $[M+H]^+$ and *m/z* 397.24 $[M-H]^-$; HRESIMS *m/z* 399.2530 $[M+H]^+$ (calculated for $C_{25}H_{35}O_4$; 399.2528) and *m/z* 421.2350 $[M+Na]^+$ (calculated for $C_{25}H_{34}NaO_4$; 421.2348).

4.6. Antimicrobial Assay

The antimicrobial activity was tested against a panel of microorganisms including bacteria: *Staphylococcus aureus* [DSM 346], *Bacillus subtilis* [DSM 10], *Acinetobacter baumanii* [DSM 30008], *Escherichia coli* [DSM 1116], *Chromobacterium violaceum* [DSM 30191], *Pseudomonas aeruginosa* [PA14] and *Mycolicibacterium smegmatis* [ATCC 700084]; and fungi: *Candida albicans* [DSM 1665], *Mucor hiemalis* [DSM 2656], *Schizosaccharomyces pombe* [DSM

70572], *Rhodotorula glutinis* [DSM 10134] and *Pichia anomala* [DSM 6766] using serial dilution assay in 96-well plates according to the previously described protocol (Becker et al., 2020). From a stock solution in methanol (1 mg/mL), the compounds were diluted in a concentration range of 66.6−0.52 µg/mL and incubated overnight with the tested strain. The MIC was then calculated as the least concentration showing no growth of the organism (clear zone). The negative control was methanol, while the positive controls were gentamycin, oxytetracycline, ciprofloxacin and kanamycin for bacteria and nystatin for fungi.

4.7. Cytotoxicity Assay

The *in vitro* cytotoxicity was evaluated using the colorimetric tetrazolium dye MTT assay against several cancerous and normal mammalian cell lines (human endocervical adenocarcinoma (KB3.1), mouse fibroblasts (L929), human lung adenocarcinoma (A549), epidermal squamous cell carcinoma (A431), breast cancer (MCF-7), prostate cancer (PC-3) and ovarian cancer (SKOV-3)), as previously described (Becker et al., 2020). Epothilone B, an FDA-approved anticancer drug acting via microtubule inhibition and cell arrest at G_2-M phase, was used as a positive control.

Conflicts of interest

There are no conflicts of interest to declare.

Acknowledgments

All authors gratefully acknowledge Prof. Dr. Marc Stadler and his research team of Microbial Drug Department at Helmholtz Center for Infection Research, Braunschweig, Germany, for hosting analytical and biological experiments. We are grateful to Wera Collisi for assistance with the antimicrobial assays, Kirsten Harmrolfs and Christel Kakoschke for performing the NMR

spectroscopic measurements, as well as Esther Surges and Aileen Gollasch for running the HRESIMS samples. S.S.E. acknowledges Alexander von Humboldt (AvH) Foundation for granting him a Georg-Forster Fellowship for Experienced Researchers (Ref 3.4-1222288-EGY-GF-E).

References

Aly, A.H., Edrada-Ebel, R., Indriani, I.D., Wray, V., Müller, W.E., Totzke, F., Zirrgiebel, U., Schächtele, C., Kubbutat, M.H., Lin, W., Proksch, P., Ebel, R., 2008. Cytotoxic metabolites from the fungal endophyte *Alternaria* sp. and their subsequent detection in its host plant *Polygonum senegalense*. J. Nat. Prod. 71, 972-980. https://doi.org/10.1021/np070447m.

Amr, K., Ibrahim, N., Elissawy, A.M., Singab, A.N.B., 2023. Unearthing the fungal endophyte *Aspergillus terreus* for chemodiversity and medicinal prospects: a comprehensive review. Fung. Biol. Biotechnol. 10, 1-33. https://doi.org/10.1186/s40694-023-00153-2.

Asmussen, B., 2012. Aboriginal vernacular names of Australian cycads of *Macrozamia*, *Bowenia* and *Lepidozamia* spp.: A response to 'Cycads in the vernacular: A compendium of local names'. Aust. Aborig. Stud. 2, 54-71.

Ayer, W.A., Racok, J.S., 1990. The metabolites of *Talaromyces flavus*: Part 1. Metabolites of the organic extracts. Can. J. Chem. 68, 2085-2094. https://doi.org/10.1139/v90-318.

Becker, K., Wessel, A.-C., Luangsa-Ard, J.J., Stadler, M., 2020. Viridistratins A-C, antimicrobial and cytotoxic benzo [j] fluoranthenes from stromata of *Annulohypoxylon viridistratum* (Hypoxylaceae, Ascomycota). Biomolecules 10, 805. https://doi.org/10.3390/biom10050805.

Benjanuwattra, J., Chaiyawat, P., Pruksakorn, D., Koonrungsesomboon, N., 2020. Therapeutic potential and molecular mechanisms of mycophenolic acid as an anticancer agent. Eur. J. Pharmacol. 887, 173580. https://doi.org/10.1016/j.ejphar.2020.173580.

Canonica, L., Kroszczynski, W., Ranzi, B., Rindone, B., Santaniello, E., Scolastico, C., 1972. Biosynthesis of mycophenolic acid. J. Chem. Soc., Perkin trans. 1, 2639-2643. https://doi.org/10.1039/P19720002639.

Chadwick, D.J., Easton, I.W., Johnstone, R.A., 1984. Fungal metabolites Part 9. Isolation and X-Ray structure determination of alternarian acid from *Alternaria mali* sp. Tetrahedron 40, 2451-2455. https://doi.org/10.1016/S0040-4020(01)83496-7.

Elsebai, M.F., 2021. Secondary metabolites from the marine-derived fungus *Phaeosphaeria spartinae*. Nat. Prod. Res. 35, 1504-1509. https://doi.org/10.1080/14786419.2019.1656623.

Gao, H., Li, G., Lou, H.X., 2018. Structural diversity and biological activities of novel secondary metabolites from endophytes. Molecules 23, 646. https://doi.org/10.3390/molecules23030646.

Joray, M.B., González, M.L., Palacios, S.M., Carpinella, M.C., 2011. Antibacterial activity of the plant-derived compounds 23-methyl-6-*O*-desmethylauricepyrone and (*Z*,*Z*)-5-(trideca-4,7-dienyl)resorcinol and their synergy with antibiotics against methicillin-susceptible and-resistant *Staphylococcus aureus*. J. Agric. Food Chem. 59, 11534-11542. https://doi.org/10.1021/jf2030665.

Kimura, Y., Yoshinari, T., Koshino, H., Fujioka, S., Okada, K., Shimada, A., 2007. Rubralactone, rubralides A, B and C, and rubramin produced by *Penicillium rubrum*. Biosci. Biotechnol. Biochem. 71, 1896-1901. https://doi.org/10.1271/bbb.70112.

Kjer, J., Debbab, A., Aly, A.H., Proksch, P., 2010. Methods for isolation of marine-derived endophytic fungi and their bioactive secondary products. Nat. Protoc. 5, 479-490. https://doi.org/10.1038/nprot.2009.233.

Liu, Y., Wu, Y., Zhai, R., Liu, Z., Huang, X., She, Z., 2016. Altenusin derivatives from mangrove endophytic fungus *Alternaria* sp. SK6YW3L. RSC Adv. 6, 72127-72132. https://doi.org/10.1039/C6RA16214B.

Mitsuhashi, S., Takenaka, J., Iwamori, K., Nakajima, N., Ubukata, M., 2010. Structure-activity relationships for inhibition of inosine monophosphate dehydrogenase and differentiation induction of K562 cells among the mycophenolic acid derivatives. Bioorg. Med. Chem. 18, 8106-8111. https://doi.org/10.1016/j.bmc.2010.09.004.

Narang, R., Kumar, R., Kalra, S., Nayak, S.K., Khatik, G.L., Kumar, G.N., Sudhakar, K., Singh, S.K., 2019. Recent advancements in mechanistic studies and structure activity relationship of FoF1 ATP synthase inhibitor as antimicrobial agent. Eur. J. Med. Chem. 182, 111644. https://doi.org/10.1016/j.ejmech.2019.111644.

Pang, X., Lin, X., Wang, P., Zhou, X., Yang, B., Wang, J., Liu, Y., 2018. Perylenequione derivatives with anticancer activities isolated from the marine sponge-derived fungus, *Alternaria* sp. SCSIO41014. Mar. Drugs 16, 280. https://doi.org/10.3390/md16080280.

Siebert, A., Wysocka, M., Krawczyk, B., Cholewiński, G., Rachoń, J., 2018. Synthesis and antimicrobial activity of amino acid and peptide derivatives of mycophenolic acid. Eur. J. Med. Chem. 143, 646-655. https://doi.org/10.1016/j.ejmech.2017.11.094.

Toghueo, R.M.K., Boyom, F.F., 2020. Endophytic *Penicillium* species and their agricultural, biotechnological, and pharmaceutical applications. 3 Biotech 10, 107. https://doi.org/10.1007/s13205-020-2081-1.

Visagie, C., Houbraken, J., Frisvad, J.C., Hong, S.-B., Klaassen, C., Perrone, G., Seifert, K., Varga, J., Yaguchi, T., Samson, R., 2014. Identification and nomenclature of the genus *Penicillium*. Stud. Mycol. 78, 343-371. https://doi.org/10.1016/j.simyco.2014.09.001.

Wang, Q.X., Bao, L., Yang, X.L., Guo, H., Yang, R.N., Ren, B., Zhang, L.X., Dai, H.Q., Guo, L.D., Liu, H.W., 2012. Polyketides with antimicrobial activity from the solid culture of an endolichenic fungus *Ulocladium* sp. Fitoterapia 83, 209-214. https://doi.org/10.1016/j.fitote.2011.10.013.

Wei, P.Y., Liu, L.X., Liu, T., Chen, C., Luo, D.Q., Shi, B.Z., 2015. Three new pigment protein tyrosine phosphatases inhibitors from the insect parasite fungus *Cordyceps gracilioides*: terreusinone A, pinophilin C and cryptosporioptide A. Molecules 20, 5825-5834. https://doi.org/10.3390/molecules20045825.

Xu, X., Zhang, X., Nong, X., Wang, J., Qi, S., 2017. Brevianamides and mycophenolic acid derivatives from the deep-sea-derived fungus *Penicillium brevicompactum* DFFSCS025. Mar. Drugs 15, 43. https://doi.org/10.3390/md15020043.

Yamaguchi, S., Nedachi, M., Maekawa, M., Murayama, Y., Miyazawa, M., Hirai, Y., 2006. Synthetic study for two 2H-chromenic acids, 8-chlorocannabiorcichromenic acid and mycochromenic acid. J. Heterocycl. Chem. 43, 29-41. https://doi.org/10.1002/jhet.5570430105.

Yang, H., Qi, B., Ding, N., Jiang, F., Jia, F., Luo, Y., Xu, X., Wang, L., Zhu, Z., Liu, X., 2019. Polyketides from *Alternaria alternata* MT-47, an endophytic fungus isolated from *Huperzia serrata*. Fitoterapia 137, 104282. https://doi.org/10.1016/j.fitote.2019.104282

Zhang, Q., Yang, B., Li, F., Liu, M., Lin, S., Wang, J., Xue, Y., Zhu, H., Sun, W., Hu, Z., 2018. Mycophenolic acid derivatives with immunosuppressive activity from the coral-derived

fungus *Penicillium bialowiezense*. Mar. Drugs 16, 230. https://doi.org/10.3390/md16070230.

Zhu, X., Liu, X., Liu, T., Wang, Y., Ahmed, N., Li, Z., Jiang, H., 2021. Synthetic biology of plant natural products: From pathway elucidation to engineered biosynthesis in plant cells. Plant Commun. 2, 100229. https://doi.org/10.1016/j.xplc.2021.100229.

Table 1. 1D (^{1}H and ^{13}C) and 2D (COSY, HMBC and ROESY) NMR data of **1**.

pos.	δ_C,[a,b] type	δ_H[c] (multi, *J*(Hz), nH)	COSY[a]	HMBC[a]	ROESY[a]
1	166.2, CO				
2	105.4, C				
3	161.5, C				
4	105.5, CH	6.59 (d, 1.9, 1H)	H-6	C-1, C-2, C-3, C-5, C-6	H_3-13
5	168.8, C				
6	99.7, CH	6.55 (br s, 1H)	H-4	C-2, C-4, C-5w[d]	H_3-13
7	147.2, C				
8	108.6, C				
9	164.1, C				
10	120.1, CH	6.29 (q, 1.6, 1H)	H_3-12	C-8, C-9, C-11, C-12	H_3-12
11	169.4, CO				
12	11.9, CH_3	1.92 (d, 1.6)	H-10	C-8, C-9, C-10, C-11w[d]	H-10
13	56.6, CH_3	3.86 (s, 3H)		C-5	

Measured in acetone-d_6 at [a] 175 and [c] 700 MHz. [b] Assignment based on *g*HMBC and *g*HMQC spectra.

[d] "w" denotes weak correlation.

Table 2. Antimicrobial assay (MIC) of isolated compounds.

Organism	Compound (MIC in µg/ml)													Reference[b] (MIC in µg/ml)
	1	**2**	**3**	**4**	**5**	**6**	**7**	**8**	**9**	**10**	**11**	**12**	**13**	
Schizosaccharomyces pombe	n.i.[a]	n.i.[a]	n.i.[a]	n.i.[a]	n.t.[b]	n.i.[a]	n.i.[a]	n.t.[b]	n.i.[a]	n.i.[a]	n.i.[a]	n.i.[a]	n.i.[a]	2.1[N]
Pichia anomala	n.i.[a]	n.i.[a]	n.i.[a]	n.i.[a]	n.t.[b]	n.i.[a]	n.i.[a]	n.t.[b]	n.i.[a]	n.i.[a]	n.i.[a]	n.i.[a]	n.i.[a]	4.2[N]
Mucor hiemalis	n.i.[a]	n.i.[a]	n.i.[a]	n.i.[a]	**66.6**	**66.6**	**66.6**	n.i.[a]	n.i.[a]	n.i.[a]	n.i.[a]	n.i.[a]	**66.6**	2.1[N]
Candida albicans	n.i.[a]	n.i.[a]	n.i.[a]	n.i.[a]	n.t.[b]	n.i.[a]	**66.6**	n.t.[b]	n.i.[a]	n.i.[a]	n.i.[a]	n.i.[a]	n.i.[a]	2.1[N]
Rhodotorula glutinis	n.i.[a]	n.i.[a]	n.i.[a]	n.i.[a]	n.t.[b]	n.i.[a]	**66.6**	n.t.[b]	n.i.[a]	n.i.[a]	n.i.[a]	n.i.[a]	n.i.[a]	2.1[N]
Acinetobacter baumanii	n.i.[a]	n.i.[a]	n.i.[a]	n.i.[a]	n.t.[b]	n.i.[a]	n.i.[a]	n.t.[b]	n.i.[a]	n.i.[a]	n.i.[a]	n.i.[a]	n.i.[a]	0.53[C]
Escherichia coli	n.i.[a]	n.i.[a]	n.i.[a]	n.i.[a]	n.t.[b]	n.i.[a]	n.i.[a]	n.t.[b]	n.i.[a]	n.i.[a]	n.i.[a]	n.i.[a]	n.i.[a]	0.83[G]
Bacillus subtilis	n.i.[a]	n.i.[a]	n.i.[a]	n.i.[a]	n.i.[a]	n.i.[a]	n.i.[a]	n.i.[a]	n.i.[a]	n.i.[a]	n.i.[a]	n.i.[a]	n.i.[a]	16.6[O]
Mycobacterium smegmatis	n.i.[a]	n.i.[a]	n.i.[a]	n.i.[a]	n.t.[b]	n.i.[a]	**66.6**	n.t.[b]	n.i.[a]	n.i.[a]	n.i.[a]	n.i.[a]	n.i.[a]	1.7[K]
Staphylococcus aureus	n.i.[a]	n.i.[a]	**2.1**	n.i.[a]	n.i.[a]	n.i.[a]	n.i.[a]	n.i.[a]	n.i.[a]	n.i.[a]	n.i.[a]	n.i.[a]	n.i.[a]	0.83[G]
Pseudomonas aeruginosa	n.i.[a]	n.i.[a]	n.i.[a]	n.i.[a]	n.t.[b]	n.i.[a]	n.i.[a]	n.t.[b]	n.i.[a]	n.i.[a]	n.i.[a]	n.i.[a]	n.i.[a]	0.21[G]
Chromobacterium violaceum	n.i.[a]	n.i.[a]	n.i.[a]	n.i.[a]	n.t.[b]	n.i.[a]	n.i.[a]	n.t.[b]	n.i.[a]	n.i.[a]	n.i.[a]	n.i.[a]	n.i.[a]	1.7[G]

[a] n.i.: no inhibition observed. [b] n.t.: not tested. [N]: Nystatin 10 mg/mL, [C]: Cirpofloxacin 2.54 mg/mL, [G]: Gentamycin 1 mg/mL, [O]: Oxytetracycline 1 mg/mL, [K]: Kanamycin 1 mg/mL.

Table 3. Cytotoxic activity (IC_{50}) of isolated compounds.

Cell line	Compound (IC_{50} in µM)													Epothilone B
	1	**2**	**3**	**4**	**5**	**6**	**7**	**8**	**9**	**10**	**11**	**12**	**13**	**(IC_{50} in nM)**
L929	n.i.[a]	n.i.[a]	54.7	n.i.[a]	23.1	58.4	**0.2**	n.i.[a]	n.i.[a]	n.i.[a]	**12.6**	n.i.[a]	n.i.[a]	0.7
KB3.1	n.i.[a]	n.i.[a]	**8.3**	n.i.[a]	26.5	81.1	**0.2**	n.i.[a]	n.i.[a]	n.i.[a]	21.6	n.i.[a]	n.i.[a]	0.2
A549	n.t.[b]	n.i.[a]	41.6	n.i.[a]	n.t.[b]	n.t.	**0.4**	n.t.[b]	n.t.[b]	n.t.[b]	20.3	n.t.[b]	n.t.[b]	0.1
A-431	n.t.[b]	n.i.[a]	n.t.[b]	n.t.[b]	n.t.[b]	n.t.	**0.1**	n.t.[b]	n.t.[b]	n.t.[b]	n.t.	n.t.[b]	n.t.[b]	0.1
PC-3	n.t.[b]	n.i.[a]	n.t.[b]	n.t.[b]	n.t.[b]	n.t.	**0.4**	n.t.[b]	n.t.[b]	n.t.[b]	**11.3**	n.t.[b]	n.t.[b]	0.1
MCF-7	n.t.[b]	n.i.[a]	n.t.[b]	n.t.[b]	n.t.[b]	n.t.	**0.1**	n.t.[b]	n.t.[b]	n.t.[b]	**3.6**	n.t.[b]	n.t.[b]	0.1
SKOV-3	n.t.[b]	n.i.[a]	n.t.[b]	n.t.[b]	n.t.[b]	n.t.	**0.1**	n.t.[b]	n.t.[b]	n.t.[b]	n.t.	n.t.[b]	n.t.[b]	0.1

[a] n.i.: no inhibition. [b] n.t.: not tested.

Legends:

Figure 1. Chemical structures of isolated compounds **1-13**

Figure 2. Key COSY, HMBC and ROESY correlations of alternatain E (**1**).

Figure 3. Experimental and calculated ECD spectra of alternatain E (**1**).

Figure 4. Key COSY and HMBC correlations of mycochromenic acid methyl ester (**2**).

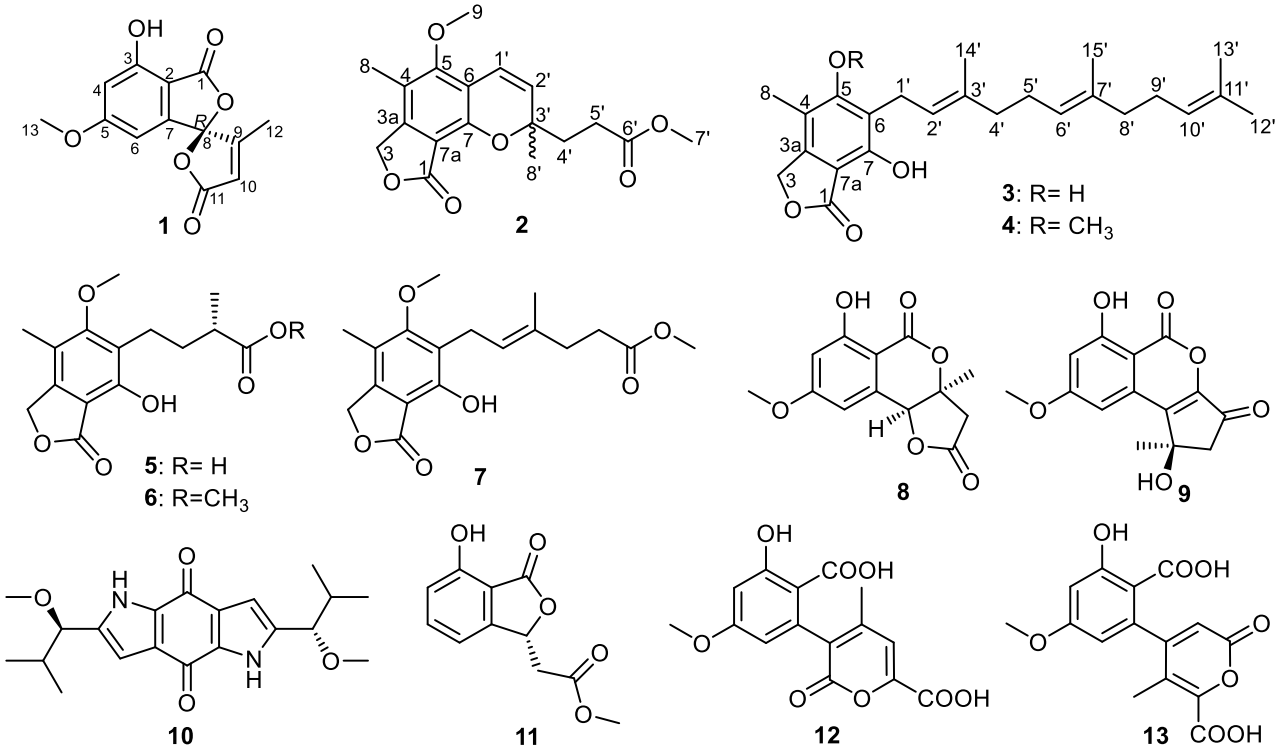

Figure 1.

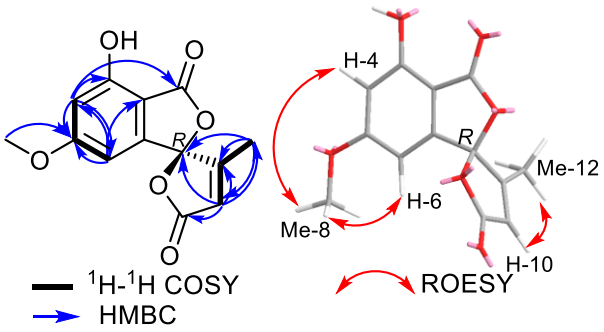

Figure 2.

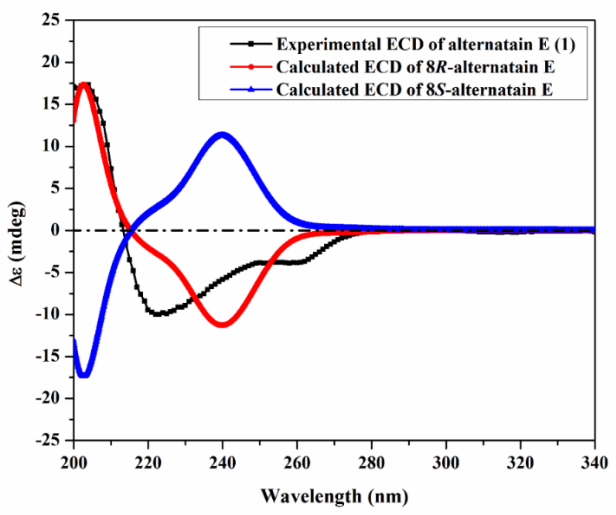

Figure 3.

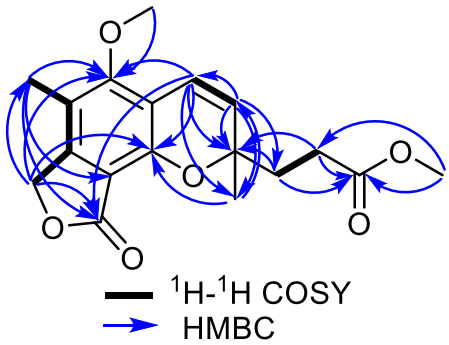

Figure 4.